Application of Magnetic Measurements for the Characterization of Topsoil Pollution in Industrial Environments

Sudarningsih Sudarningsih
Department of Physics, Faculty of Mathematics and Natural Sciences, Universitas Lambung Mangkurat, Banjarbaru, Indonesia
sudarningsih@ulm.ac.id (corresponding author)

Tetti Novalina Manik
Department of Physics, Faculty of Mathematics and Natural Sciences, Universitas Lambung Mangkurat, Banjarbaru, Indonesia
tetti.manik@ulm.ac.id

Ibrahim Ibrahim
Department of Physics, Faculty of Mathematics and Natural Sciences, Universitas Lambung Mangkurat, Banjarbaru, Indonesia
Ibrahimsota@ulm.ac.id

Abd Mujahid Hamdan
Department of Environmental Engineering, Faculty of Science and Technology, Universitas Islam Negeri Ar-Raniry Banda Aceh, Banda Aceh, Indonesia
abd.mujahid.hamdan@gmail.com

Hamdi Rifai
Department of Physics, Faculty of Mathematics and Natural Sciences, Universitas Negeri Padang, Padang, Indonesia
rifai.hamdi@gmail.com

Siti Zulaikah
Department of Physics, Faculty of Mathematics and Natural Sciences, Universitas Negeri Malang, Malang, Indonesia
siti.zulaikah.fmipa@um.ac.id

Ikbal Setiawan
Department of Physics, Faculty of Mathematics and Natural Sciences, Universitas Lambung Mangkurat, Banjarbaru, Indonesia
1811014210019@mhs.ulm.ac.id

Ella Rachmah Dwi Putri
Department of Physics, Faculty of Mathematics and Natural Sciences, Universitas Lambung Mangkurat, Banjarbaru, Indonesia
211014120009@mhs.ulm.ac.id

Laela Azizah
Department of Physics, Faculty of Mathematics and Natural Sciences, Universitas Lambung Mangkurat, Banjarbaru, Indonesia
2111014220006@mhs.ulm.ac.id

Received: 17 July 2025 | Revised: 3 September 2025 | Accepted: 15 September 2025

 DOI: https://doi.org/10.48084/etasr.13459

ABSTRACT

This study aims to examine the feasibility of using magnetic techniques to identify anthropogenic materials produced by human activities. Rock magnetism, geochemical analysis, and pollution index calculations were used. The magnetic signal of the topsoil from the industrial area is greatly enhanced when compared with the background, with a magnetic susceptibility (χ_{LF}) of 0.23–42.60 × 10^{-6} m^3/kg. However, industrial topsoil contains only a small number of pedogenic Superparamagnetic (SP) grains, as indicated by the low average χ_{FD}% value (<2%). The geochemical properties of the magnetic fraction in industrial topsoil differ significantly from those of topsoil generally found in peatlands. This indicates that magnetic minerals in industrial topsoil originate not only from pedogenic processes, but also from parent soil materials in the surrounding area. Significant magnetic correlation techniques can screen for topsoil pollution in this area, as evidenced by the significant correlations between χ_{LF}, Fe, and Mn, as well as between χ_{HF} and χ_{FD}%. Five heavy metals had abundances exceeding the threshold, as shown by the Pollution Load Index (PLI), which indicated moderate to very high pollution.

Keywords-peatland; monitoring; lithogenic; anthropogenic; geochemistry

I. INTRODUCTION

The soil surface contains various elements, including heavy metals. These elements can be natural (lithogenic) or the result of human activities (anthropogenic) [1]. Urban areas are particularly vulnerable to heavy metal contamination [2]. According to [3], the industrial area has the potential to be polluted, with increased concentrations of heavy metals appearing in many industrial and urban soils [2]. Since heavy metals do not decompose, they can accumulate in soil, and the latter is not a renewable natural resource. It is, thus, required to monitor heavy metal concentrations in soil to prevent pollution and propose remediation actions if necessary [4]. There are two possible ways to identify magnetic particles in heavy metal pollution: heavy metals entering the crystal structure during combustion or particle formation and heavy metals being adsorbed into magnetic particles after particle formation [5]. Indirectly, this explains that the presence of anthropogenically produced magnetic particles also indicates the presence of heavy metals. Therefore, magnetic measurements (magnetic susceptibility) have become an important tool for estimating anthropogenic heavy metal pollution in soil [6] and sediment [7]. Additionally, magnetic susceptibility is a cost-effective, rapid, and non-destructive measurement method. Several studies report a positive correlation between magnetic susceptibility and the level of heavy metal pollution in industrial areas. This method is widely accepted for estimating the levels of heavy metal pollution. The values of magnetic susceptibility reveal the concentration and granulometric distribution of ferromagnetic minerals, such as magnetite and maghemite, coming from natural processes or human activities. The frequency-dependent magnetic susceptibility percentage value was used to distinguish between naturally occurring and anthropogenically produced ferromagnetic minerals. Naturally produced ferromagnetic minerals are ultrafine SP particles (<0.03 μm) that are frequency dependent. In contrast, anthropogenically produced ferromagnetic particles are Multidomain (MD) and Stable Single-Domain (SSD) magnetic particles that are independent of frequency [8]. Consequently, many studies have used soil's magnetic susceptibility to map the spatial distribution of heavy metal pollution economically. However, no research examining the heavy metal content or increase in magnetic susceptibility of the top layer of soil in industrial areas of Banjarmasin has been conducted. The main objectives of this study are to: evaluate the heavy metal content and pollution level in the surface soil of industrial areas in the city, determine the distribution of heavy metals and their magnetic susceptibility, and correlate metal pollution with magnetic susceptibility.

II. MATERIALS AND METHODS

Banjarmasin City is located between latitudes 3°16'46" and 3°22'54" south and longitudes 114°31'40" and 114°39'55" east, as presented in Figure 1. The city's industrial area is located to the west, including plywood manufacturing, household furniture production, palm oil processing, and warehousing. The industrial area is located on the banks of the Martapura and Barito rivers, in a swampy area that geologically consists of alluvium [9].

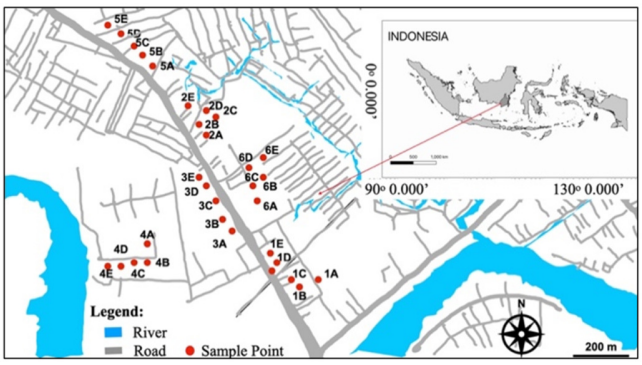

Fig. 1. Map of the study area showing the sampling sites (red dots).

In the study area, a total of 30 topsoil samples were numbered 1A–1E, 2A–2E, and 6A–6E based on their respective locations. A plastic shovel was used to collect five soil samples at depths ranging from 5 cm to 15 cm, subsequently storing them in a plastic bag at each designated location. The vehicle's location was subsequently documented through GPS tracking. The procedure entails the air-drying of the soil samples at ambient temperature within the laboratory setting. Authors in [10] outlined that the soil samples were sifted through a 2-mm sieve following the drying process. For the magnetic susceptibility testing, specific samples were meticulously positioned within a cylindrical plastic holder, measuring 25.4 mm in length and 22 mm in width. In accordance with the methodology established in [11], a subset of the residual bulk samples was used to quantify the metal content. Thereafter, a magnetic stirrer was employed to facilitate the magnetic separation of the samples from each respective location. The extraction of magnetic particles was achieved through the application of a rotating magnetic field, generated by a magnet wrapped in parafilm, within a soil-water solution (1:10). To ensure the collection of magnetic particles, the parafilm was detached from the magnet and thoroughly rinsed with deionized water, a process repeated until no magnetic particles remain. A thorough examination of the magnetic mineral crystal structures, shapes, and sizes of the extracted samples was conducted. The identification of crystal structures and magnetic mineral grain shapes and sizes was facilitated by the usage of XRD and SEM. The range of the magnetic mineral grains in the SD category is from 0.03 μm to 0.1 μm, in the PSD category from 0.1 μm to 20 μm, and in the MD category from >20 μm [12]. A specially designed meter (Bartington Instrument Ltd., Oxford, UK) was used to assess the magnetic susceptibility of the samples under consideration, exhibiting an accuracy of 1%. The values of low-frequency magnetic susceptibility (χ_{LF}), high-frequency magnetic susceptibility (χ_{HF}), and frequency-dependent magnetic susceptibility (χ_{FD}) were calculated by [12]:

$$\chi_{FD}(\%) = \frac{\chi_{LF} - \chi_{HF}}{\chi_{LF}} \times 100\% \quad (1)$$

The metal content present in the soil samples was measured using a PANalytical X-ray fluorescence instrument, model: Minipal 4. The crystal structure was analyzed using a Rigaku-SmartLab X-ray diffractometer, and a Scanning Electron Microscope Energy Dispersive Spectroscopy (SEM-EDS) analysis was conducted using a JED-2300T Energy Dispersion X-ray spectrometer to observe the shape and size of the magnetic minerals of the extracted samples. The statistical analysis of the data was conducted using the SPSS Statistics 20.0 for Windows program, while a one-way Analysis of Variance (ANOVA) was used to assess the variability present within the soil layers. The relationship between the magnetic characteristics and the geochemical index was examined using a Pearson correlation analysis. The Geoaccumulation Index (I_{geo}) was used to compare the concentrations of heavy metals in research samples to the metal content in a reference sample [13]:

$$I_{geo} = log_2\left(\frac{C_n}{1.5B_n}\right) \quad (2)$$

where C_n is the metal content in the research sample, B_n is the background value of the metal in question, and 1.5 is the background matrix correction factor that causes lithogenic influence. Authors in [13] showed that I_{geo} is divided into classes: first ($I_{geo} \leq 0$, Class 0) for uncontaminated categories, second (I_{geo} 0‑1, Class 1) for uncontaminated to moderately contaminated categories, third (I_{geo} 1 ‑ 2, Class 2) for moderately contaminated categories, fourth (I_{geo} 2–3 Class 3) for moderate to highly contaminated categories, fifth (I_{geo} 3–4, Class 4) for highly to very highly contaminated categories, and sixth (I_{geo} 4–5, Class 5) for very highly contaminated categories.

III. RESULTS AND DISCUSSION

Table I presents the findings of the measurements of χ_{LF}, χ_{HF}, and χ_{FD}. The χ_{LF} value ranges from (0.23 - 42.60) × 10-6 m^3/kg, with an average value of 7.27 × 10-6 m^3/kg. The χ_{FD} value ranges from 0.28 to 4.16, with an average value of 1.29. The findings from these analyses suggest the presence of variations in the values at each sampling point. As indicated by the data presented in Table I, point 3D exhibited the highest susceptibility value, which increased significantly when compared to points 3C and 3E. The value of χ_{FD} underwent a substantial alteration at point 3D in comparison to points 3C and 3E. The elevated standard deviation observed in the magnetic susceptibility measurements signifies substantial variability within the examined domain. Table I also displays the average value of χ_{FD} (%), ranging from 0.28% to 4.16%, with an average value of 1.29%. Metal concentrations indicated the presence of titanium (Ti), vanadium (V), chromium (Cr), manganese (Mn), iron (Fe), nickel (Ni), copper (Cu), and zinc (Zn) in each soil sample. The specimen with the highest Fe content is displayed in three dimensions. As presented in sample 3B, the highest values for titanium (Ti) and vanadium (V) metals are evident. Sample 1E exhibits the greatest quantity of chromium, manganese, and copper. Other samples with the highest content are 1A (Ni), and 3C (Zn). This underscores the intricate nature of metal enrichment mechanisms within surface soil. Figure 2, presents the diffractogram from the XRD measurements for the 3D sample. The objective of XRD analysis is to ascertain the nature of the magnetic mineral present in the specimen. The diffractogram indicates that the minerals present in the extraction sample are composed of magnetite, quartz, nacrite, anorthite, sodalite, and saponite. The mineralogical analysis of the samples revealed the presence of magnetite, a strongly ferromagnetic mineral. Figure 3 presents the outcomes of the SEM-EDS analysis. The findings corroborate the results of the XRD diffractogram with respect to minerals. These elements include Mg, Si, Fe, Al, and O. There are six minerals made up of these elements: saponite ($Ca_{0.1}Na_{0.1}Mg_{2.25}Fe^{2+}_{0.75}Si_3AlO_{10}(OH)_2 \bullet 4(H_2O)$, nacrite ($Al_2Si_2O_5(OH)_4$), anorthite ($CaAl_2Si_2O_8$), sodalite ($Na_8(Al_6Si_6O_{24})\ Cl_2$), and quartz ($SiO_2$). Table II presents the analyses of the geoaccumulation indices, indicating that Ti, V, Mn, and Fe did not pollute any soil sample. The presence of Cu was detected in every sample. Cr and Ni were detected in all samples, with the exception of sample 3D. In contrast, Zn was detected in all samples except sample 1A. Samples 1A (I_{geo} = 4.7) and 1B exhibited Ni concentrations that were found to be

significantly contaminated. It was determined that sample 1E (I_{geo} = 3.2) exhibited high levels of Cr pollution. Samples 1B (I_{geo} =3.1), 2A (I_{geo} =3.8), 5A (I_{geo} =3.1), 5B (I_{geo} =3.0), 5C (I_{geo} =3.7), and 6D (I_{geo} =3.5) were highly contaminated with Ni, while samples 1E (I_{geo} = 3.3) and 5E (I_{geo} = 3.1) were highly contaminated with Cu. Samples 2B (I_{geo} =3.4) and 3B (I_{geo} =3.8) exhibited elevated levels of Zn contamination.

TABLE I. METAL CONCENTRATIONS AND MAGNETIC SUSCEPTIBILITY MEASUREMENT DATA IN THE TOPSOIL SAMPLES

Sample/site	Metal concentration (mg/kg) ×103								χ_{LF}	χ_{HF}	χ_{FD}
	Ti	V	Cr	Mn	Fe	Ni	Cu	Zn	(× 10^{-6} m^3/ kg)		(%)
1A	0.61	0.05	0.86	0.73	46.80	2.66	0.22	0.14	9.47	9.44	0.28
1B	0.79	0.06	0.70	0.58	40.40	0.87	0.26	0.23	10.20	10.10	0.55
1C	1.17	0.08	0.84	0.53	29.60	0.75	0.17	0.28	6.09	6.05	0.68
1D	2.57	0.15	0.31	0.30	35.10	0.20	0.19	0.25	1.17	1.16	0.76
1E	0.88	0.04	1.27	0.88	44.10	0.67	0.65	2.42	4.67	4.64	0.71
2A	0.57	0.04	0.67	0.51	40.80	1.42	0.20	0.45	11.1	11.0	0.57
2B	0.94	0.07	0.76	0.52	40.30	0.97	0.22	1.49	6.69	6.64	0.66
2C	0.74	0.04	0.94	0.55	32.10	0.92	0.17	0.15	6.94	6.91	0.31
2D	1.61	0.07	0.97	0.49	25.00	0.73	0.18	0.73	7.31	7.22	1.34
2E	2.53	0.16	0.43	0.30	33.30	0.37	0.20	0.28	1.03	1.02	1.08
3A	2.44	0.11	0.52	0.58	35.10	0.27	0.46	2.39	8.89	8.61	3.14
3B	6.11	0.17	0.24	0.47	23.40	0.12	0.48	1.96	10.70	10.30	3.15
3C	1.20	0.06	0.28	0.32	32.80	0.23	0.21	3.43	9.79	9.63	1.55
3D	1.10	0.06	0.11	0.59	55.50	0.05	0.13	0.21	42.60	40.80	4.16
3E	0.94	0.13	0.84	0.40	33.90	0.74	0.17	0.15	8.21	8.16	0.59
4A	2.71	0.04	0.56	0.28	23.90	0.35	0.18	0.17	2.74	2.67	2.58
4B	0.89	0.04	0.63	0.37	33.50	0.76	0.19	0.33	8.12	8.07	0.56
4C	0.90	0.04	0.63	0.34	26.20	0.54	0.16	0.16	5.71	5.68	0.55
4D	1.30	0.06	0.68	0.48	40.30	0.78	0.23	0.51	7.38	7.30	1.05
4E	1.03	0.04	0.56	0.37	28.90	0.58	0.18	0.26	6.03	5.99	0.70
5A	1.06	0.09	0.68	0.47	41.40	0.89	0.21	0.15	5.44	5.38	1.08
5B	1.11	0.08	0.92	0.39	35.20	0.84	0.19	0.20	6.00	5.97	0.62
5C	1.94	0.06	0.57	0.36	34.70	1.32	0.17	0.17	6.67	6.64	0.48
5D	2.21	0.09	0.35	0.23	31.10	0.29	0.15	0.09	1.51	1.49	1.54
5E	2.04	0.05	0.55	0.36	29.00	0.33	0.58	0.94	7.66	7.53	1.71
6A	3.21	0.12	0.18	0.26	25.40	0.11	0.14	0.05	0.23	0.22	3.92
6B	2.38	0.08	0.40	0.21	31.40	0.23	0.17	0.17	1.25	1.24	0.76
6C	2.03	0.11	0.48	0.40	37.70	0.39	0.23	0.31	3.66	3.60	1.69
6D	0.97	0.07	0.66	0.45	44.22	1.17	0.18	0.18	6.01	5.96	0.85
6E	2.11	0.08	0.49	0.37	32.70	0.41	0.19	0.35	4.96	4.92	0.92
Min	0.57	0.04	0.11	0.21	23.40	0.05	0.13	0.05	0.23	0.23	0.28
Max	6.11	0.17	1.27	0.88	55.50	2.66	0.65	3.43	42.60	40.80	4.16
Average	1.67	0.08	0.60	0.44	34.79	0.67	0.23	0.62	7.27	7.15	1.29
Std. Dev.	1.11	0.04	0.26	0.15	7.37	0.52	0.13	0.85	7.32	7.02	1.06
Earth crust [14]	4.60	0.13	0.09	0.85	47.20	0.07	0.05	0.10	-	-	-

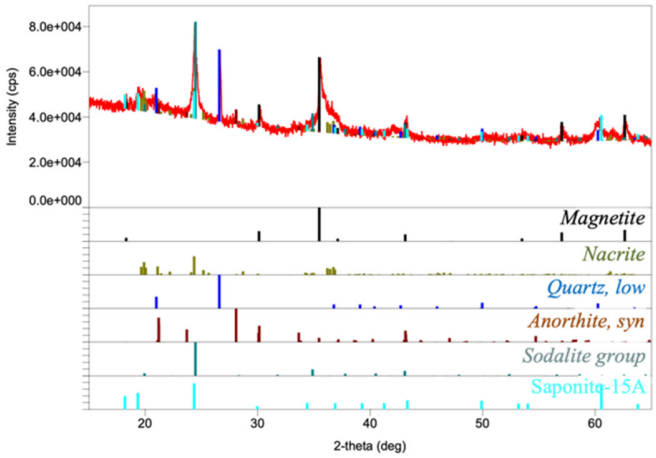

Fig. 2. XRD diffractogram for surface soil sample from point 3E.

The χ_{LF} value from the research area is higher than values from other industrial areas, including those from Shanghai, China [15], Jos Metropolis, Nigeria [16], and lower than values from Ilorin, Nigeria [17]. The Yangtze River's sedimentation produces an alluvium formation, as evidenced by the rock formations observed in other regions [11]. However, the research area in question is characterized by the presence of alluvial deposits, which comprise the soil derived from the surrounding region. This area is distinguished by the presence of bedrock, including granite, metamorphic rock, ophiolite, and sediment [12]. A study of the river sediments from the research area revealed that the χ_{LF} values range from (131.91 to 1403.64) × 10^{-8} m^3/kg) [14], which are not significantly different from the values obtained in this research area. The agricultural soils within the research area exhibit χ_{LF} values ranging from (1.10 to 136.50) × 10^{-8} m^3/kg) [18]. The high χ_{LF} value at the study site indicates that a combination of naturally formed and human-made magnetic materials likely contribute to the magnetic quality. Authors in [19] used the χ_{FD} value to identify the presence of SP particles. The χ_{FD} value on the

surface soil of the research area ranges between 0.28% and 4.16%, indicating that the sediment contains a mixture of coarse non-SP grains and fine SP grains. The soil samples were subjected to XRD analysis, which revealed that the magnetite (Fe_3O_4) peaks exhibited the most significant characteristics.

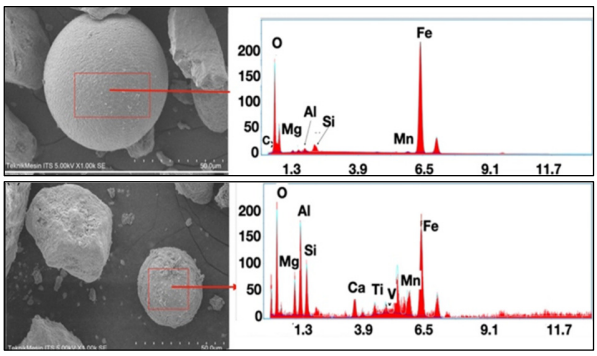

Fig. 3. The shape and size of the sample's magnetic mineral grains: (a) 3D and (b) 3E.

TABLE II. METAL GEOACCUMULATION INDEXES

Site	Geoaccumulation index							
	Ti	V	Cr	Mn	Fe	Ni	Cu	Zn
1A	-3.5	-1.9	2.7	-0.8	-0.6	4.7	1.7	-0.1
1B	-3.1	-1.6	2.4	-1.1	-0.8	3.1	1.9	0.7
1C	-2.6	-1.3	2.6	-1.3	-1.3	2.9	1.3	1.0
1D	-1.4	-0.4	1.2	-2.1	-1.0	1.0	1.5	0.8
1E	-2.9	-2.3	3.2	-0.5	-0.7	2.7	3.3	4.1
2A	-3.6	-2.3	2.3	-1.3	-0.8	3.8	1.6	1.7
2B	-2.9	-1.6	2.5	-1.3	-0.8	3.3	1.7	3.4
2C	-3.2	-2.3	2.8	-1.2	-1.1	3.2	1.3	0.1
2D	-2.1	-1.5	2.8	-1.4	-1.5	2.8	1.4	2.4
2E	-1.4	-0.3	1.7	-2.1	-1.1	1.9	1.6	1.0
3A	-1.5	-0.8	1.9	-1.1	-1.0	1.4	2.8	4.1
3B	-0.2	-0.2	0.8	-1.4	-1.6	0.2	2.8	3.8
3C	-2.5	-1.7	1.1	-2.0	-1.1	1.2	1.6	4.6
3D	-2.6	-1.7	-0.3	-1.1	-0.3	-1.0	0.9	0.6
3E	-2.9	-1.7	2.6	-1.7	-1.1	2.9	1.3	0.1
4A	-1.3	-0.6	2.1	-2.2	-1.6	1.8	1.4	0.2
4B	-2.9	-2.3	2.3	-1.8	-1.1	2.9	1.5	1.2
4C	-2.9	-2.3	2.2	-1.9	-1.4	2.4	1.2	0.2
4D	-2.4	-1.7	2.3	-1.4	-0.8	2.9	1.8	1.8
4E	-2.7	-2.3	2.1	-1.8	-1.3	2.5	1.4	0.9
5A	-2.7	-1.2	2.3	-1.4	-0.8	3.1	1.6	0.1
5B	-2.6	-1.3	2.8	-1.7	-1.0	3.0	1.5	0.5
5C	-1.8	-1.7	2.1	-1.8	-1.0	3.7	1.3	0.2
5D	-1.6	-1.1	1.4	-2.5	-1.2	1.5	1.1	-0.7
5E	-1.8	-1.9	2.0	-1.8	-1.3	1.7	3.1	2.7
6A	-1.1	-0.7	0.4	-2.3	-1.5	0.1	1.0	-1.5
6B	-1.5	-1.3	1.6	-2.6	-1.2	1.2	1.3	0.2
6C	-1.8	-0.8	1.8	-1.7	-0.9	1.9	1.8	1.1
6D	-2.8	-1.5	2.3	-1.5	-0.7	3.5	1.4	0.3
6E	-1.7	-1.3	1.9	-1.8	-1.1	2.0	1.5	1.3
Min	-3.2	-2.2	-1.2	-0.2	0.8	1.8	2.8	3.8
Max	-0.2	-0.2	3.2	-0.5	-0.3	4.7	3.3	4.6
Average	-2.3	-1.5	2.0	-1.6	-1.0	2.3	1.7	1.2
Std. Dev.	0.8	0.6	0.8	0.5	0.3	1.2	0.6	1.5

These data suggest that magnetite minerals comprise the majority of surface soil samples at this location. The SEM-EDS results indicate the presence of magnetite crystals in the sample, exhibiting a specific morphology. The formation of these minerals occurs as a result of the erosion of magnesium (Mg)-rich rocks by basic or ultrabasic acids, or through the interaction of fluids and igneous materials in a hydrothermal environment [20]. Sodalite minerals are formed by the weathering of igneous rock [21]. The spherical magnetite mineral grains indicate anthropogenic processes, according to prior investigations [22]. Table II presents the descriptive statistics for the eight elements of this study, including minimum, mean, maximum, and standard deviation, providing reference values for the metals under study, which are the earth's crust average [13]. The research area exhibits an average metal content that exceeds the earth's crust: Cr, Ni, Cu, and Zn. A comparison of the sample's data with existing industrial soil assessment standards reveals that the sample exhibits elevated levels of heavy metals, including Fe, Cr, Ni, Cu, and Zn [23, 24]. The analysis of geospatial data has revealed the presence of contamination in nearly all of the samples examined. Research suggests that the combustion of industrial coal results in the enrichment of soil metals, including chromium (Cr), copper (Cu), and nickel (Ni) [25]. Additionally, the transportation industry facilitates the deposition and enrichment of Zn in soil. Authors in [26] found that automobile tires significantly increased Zn accumulation in urban surface soils. Authors in [27] explained, that their machine learning model shows that motor vehicle exhaust particles alter air quality depending on temperature, humidity, and wind speed. The analysis of the $I_{geo} > 1$, indicates the influence of human activities, with the majority of the samples collected at the research location exhibiting $I_{geo} > 1$ values for Cr, Ni, Cu, and Zn. Authors in [28, 29] found that the average I_{geo} values for Cr, Ni, Cu, and Zn were lower in Aurangabad (India) and Bengaluru (India). Authors in [30] showed that the contamination of groundwater can be attributed not only to soil, but also to industrial activities. Table III presents the correlation coefficients between heavy metals in surface soil at the site. The presence of notable relationships signifies the existence of analogous underlying factors responsible for their genesis and deposition. The elements Zn, Cr, Mn, and Cu show a high correlation, suggesting that soil contamination in this area may be attributable to motor vehicle emissions and industrial activities. Furthermore, Table III demonstrates a substantial correlation between magnetic parameters (χ_{LF}, χ_{HF}, and χ_{FD} (%)) and elements such as Fe, Ti, Cr. Authors in [4] also reported a positive and significant correlation between χ_{LF} and Fe in soil samples from industrial areas. Furthermore, authors in [15] discovered a strong and positive correlation between χ_{LF} and Fe, as well as Mn in soil samples collected from industrial areas in Shanghai, China. According to [11], χ_{FD} (%) is indicative of the potential presence of SP mineral fractions. Authors in [31] showed that a low χ_{FD} percentage value indicates that minimal magnetic material from the soil contributes to the development of susceptibility in the soil in this research area. The study's findings indicate that the usage of χ_{LF}, χ_{HF}, and χ_{FD} (%) allows for the estimation of the Fe content, as well as Ti, Cr, and Ni content in soil within the specified research domain. In the research area, χ_{LF}, χ_{HF}, and χ_{FD} (%) are indicators of heavy metal contamination (Fe, Ti, Cr, and Ni) in the soil from anthropogenic sources. This relationship indicates that ferrimagnetic minerals are the

primary factors determining soil's magnetic susceptibility [18]. A strong correlation has been identified between χ_{FD} (%) and Cr, caused by the addition of Cr to the lattice structure of ferrimagnetic minerals during their formation and release process, or by the uptake of Cr by ferrimagnetic minerals in the environment [9]. This finding indicates that anthropogenic pollution is the primary contributing factor to the observed changes in χ_{LF} within topsoil.

TABLE III. PEARSON RELATIONSHIP BETWEEN MAGNETIC CHARACTERISTICS X_{LF}, X_{HF}, AND X_{FD} (%) AND HEAVY METALS OF SOIL IN RESEARCH LOCATION

	Ti	**V**	**Cr**	**Mn**	**Fe**	**Ni**	**Cu**	**Zn**	χ_{LF}	χ_{HF}	χ_{FD}
Ti	1	0.7	-0.6	-0.4	-0.5	-0.5	0.3	0.2	-0.2	-0.2	-0.6
V		1	-0.4	-0.2	-0.2	-0.4	0.0	0.0	-0.2	-0.2	0.3
Cr			1	0.6	0.1	0.6	0.2	0.0	-0.2	-0.2	-0.6
Mn				1	0.6	0.5	0.5	0.3	0.4	0.4	-0.1
Fe					1	0.4	0.0	0.0	0.6	0.6	-0.1
Ni						1	-0.1	-0.2	0.0	0.0	-0.6
Cu							1	0.6	0.0	0.0	0.2
Zn								1	0.1	0.1	0.2
χ_{LF}									1	1	0.4
χ_{HF}										1	0.4
χ_{FD}											1

This study offers a comparative analysis with earlier regional studies, particularly regarding the influence of lithology and mineralogy from areas external to the study area. The most compelling discovery is that the magnetic properties of the soil in the study area are affected by both the inherent characteristics of the site and the surrounding materials. Given the nature of the research site, which is a marsh containing materials from outside the area, the parent material's lithology and mineralogy are significant factors. Most studies in this field tend to concentrate on contaminants and geological elements within the specified area. The present study also identified a strong correlation between magnetic characteristics and Fe and Mn concentrations, suggesting that early surveillance in analogous locations could be more precise and effective. Magnetic characteristics have been linked to heavy metal pollution; however, this work demonstrates a more precise relationship with Fe and Mn, which could assist researchers in developing more customized monitoring systems. Research in other industrial areas reveals elevated magnetic values in areas contaminated by industrial and traffic pollutants. This research corroborates extant theories and introduces a novel dimension by demonstrating how the geological context and sources of material outside the study site can substantially influence geophysical readings.

IV. CONCLUSIONS

The present study uses surface soil samples extracted from industrial areas in South Kalimantan, Indonesia, to examine the relationship between the concentrations of specific heavy metals and magnetic properties. The study site exhibited elevated concentrations of heavy metals and magnetic susceptibility values that exceeded established thresholds, as evidenced by comprehensive magnetic property measurements and geochemical tests. In this study, the χ_{LF}, χ_{HF}, and χ_{FD} (%) of the tested soil exhibited significant correlations with Fe and Mn contents. Concurrently, five of the heavy metals under analysis in the study area showed concentrations that exceeded the established threshold, as indicated by the Pollution Load Index (PLI), which exhibited moderate to very high levels of pollution. A finding of the study is the observation that the lithology and mineralogy of the parent material in the study area exert minimal influence on the χ_{LF}, χ_{HF}, and χ_{FD} (%) values in the soil. However, the lithology and minerals of the parent material from the surrounding area are found to be highly significant in this regard. This significance arises from the fact that the study area is characterized by a swampy environment, with soil material originating from the surrounding area. The enrichment of χ_{LF}, χ_{HF}, and χ_{FD} (%) values and heavy metal content are also suspected to originate from industrial activities and vehicle traffic, both land and river. The study's findings suggest that magnetic parameters (χ_{LF}, χ_{HF}, and χ_{FD} (%)) can be used to predict the presence of heavy metals Fe and Mn at the research site and in analogous locations.

ACKNOWLEDGMENT

The authors are thankful to reviewers and editors for their constructive comments. This research was financially supported by a research grant (Hibah Penelitian Padanan Dalam Negeri) to Sudarningsih from Universitas Lambung Mangkurat, Indonesia (1374.105/UN8.2/PG/2024).

REFERENCES

[1] B. J. Alloway, "Sources of Heavy Metals and Metalloids in Soils," in *Heavy Metals in Soils: Trace Metals and Metalloids in Soils and their Bioavailability*, B. J. Alloway, Ed. Dordrecht: Springer Netherlands, 2013, pp. 11–50.

[2] P. N and R. C. R, "Heavy Metal Analysis and Health Risk Assessment of Groundwater and Soil in and Around Peenya Industrial Area, Bengaluru," *Ecological Engineering & Environmental Technology*, vol. 25, no. 7, pp. 63–79, July 2024, https://doi.org/10.12912/27197050/188008.

[3] N. Harkat, A. Rahmane, and I. Bendjemila, "The Impact of Industrial Air Pollution on the Urban Environment of Setif: Modeling and Mapping of Total Suspended Particles," *Engineering, Technology & Applied Science Research*, vol. 12, no. 6, pp. 9431–9439, Dec. 2022, https://doi.org/10.48084/etasr.5256.

[4] M. H. Salehi, S. Jorkesh, and R. Mohajer, "Relationship between Magnetic Susceptibility and Heavy Metals Concentration in Polluted Soils of Lenjanat Region, Isfahan," *E3S Web of Conferences*, vol. 1, 2013, Art. no. 04003, https://doi.org/10.1051/e3sconf/20130104003.

[5] U. Kukier, C. F. Ishak, M. E. Sumner, and W. P. Miller, "Composition and element solubility of magnetic and non-magnetic fly ash fractions," *Environmental Pollution*, vol. 123, no. 2, pp. 255–266, May 2003, https://doi.org/10.1016/S0269-7491(02)00376-7.

[6] S. Sudarningsih, T. N. Manik, F. Fahruddin, G. Tamuntuan, F. Razi, and D. Dzikri, "Identification of Anthropogenic Materials in Topsoil from the Urban Area of Banjarmasin, Indonesia Using Geochemical and Rock Magnetic Properties," *Rudarsko-geološko-naftni zbornik*, vol. 40, no. 4, pp. 1–14, Aug. 2025, https://doi.org/10.17794/rgn.2025.4.1.

[7] R. Maity, M. Venkateshwarlu, S. Mondal, M. R. Kapawar, D. Gain, and P. Paul, "Magnetic and microscopic characterization of anthropogenically produced magnetic particles: a proxy for environmental pollution," *International journal of environmental science and technology*, vol. 18, no. 7, pp. 1793–1808, 2021.

[8] S. Ayoubi, M. J. Samadi, H. Khademi, M. Shirvani, and Y. Gyasi-Agyei, "Using magnetic susceptibility for predicting hydrocarbon pollution levels in a petroleum refinery compound in Isfahan Province, Iran," *Journal of Applied Geophysics*, vol. 172, Jan. 2020, Art. no. 103906, https://doi.org/10.1016/j.jappgeo.2019.103906.

[9] N. Sikumbang and R. Heryanto, *Geological Map of Banjarmasin Sheet*. Bandung, Indonesia: Center for Geological Research and Development, 1994.

[10] X. Zhang *et al.*, "Soil Quality Assessment in Farmland of a Rapidly Industrializing Area in the Yangtze Delta, China," *International Journal of Environmental Research and Public Health*, vol. 19, no. 19, Jan. 2022, Art. no. 12912, https://doi.org/10.3390/ijerph191912912.

[11] J. Zhang, L. Liu, X. Wei, Y. Sun, L. Wang, and X. Xie, "Effectiveness of magnetic separation pretreatment methods in evaluating heavy metal pollution in urban soils: a case study of Nanjing City," *Environmental Geochemistry and Health*, vol. 47, no. 7, June 2025, Art. no. 240, https://doi.org/10.1007/s10653-025-02558-x.

[12] J. A. Dearing, *Environmental magnetic susceptibility : using the Bartington MS2 system*. Kenilworth, Warwickshire, UK: Chi Publishing, 1994.

[13] G. Muller, "Index of geoaccumulation in sediments of the rhine river," *GeoJournal*, vol. 2, no. 3, pp. 108–118, Jan. 1969.

[14] K. K. Turekian and K. H. Wedepohl, "Distribution of the Elements in Some Major Units of the Earth's Crust," *Geological Society of America Bulletin*, vol. 72, no. 2, 1961, Art. no. 175, https://doi.org/10.1130/0016-7606(1961)72%255B175:DOTEIS%255D2.0.CO;2.

[15] G. Wang *et al.*, "Magnetic evidence for heavy metal pollution of topsoil in Shanghai, China," *Frontiers of Earth Science*, vol. 12, no. 1, pp. 125–133, Mar. 2018, https://doi.org/10.1007/s11707-017-0624-5.

[16] E. S. Akanbi and E. J. Nasamu, "Magnetic Pollution of Soil Samples at Some Industrial Sites in Jos Metropolis, Plateau State, Nigeria," *Journal of Applied Sciences and Environmental Management*, vol. 24, no. 2, pp. 193–196, Apr. 2020, https://doi.org/10.4314/jasem.v24i2.1.

[17] M. M. Orosun, S. A. Oniku, A. Peter, R. O. Orosun, N. B. Salawu, and L. Hitler, "Magnetic susceptibility measurement and heavy metal pollution at an automobile station in Ilorin, North-Central Nigeria," *Environmental Research Communications*, vol. 2, no. 1, Jan. 2020, Art. no. 015001, https://doi.org/10.1088/2515-7620/ab636a.

[18] S. Sudarningsih *et al.*, "Assessment of Soil Contamination by Heavy Metals: A Case of Vegetable Production Center in Banjarbaru Region, Indonesia," *Polish Journal of Environmental Studies*, vol. 32, no. 1, pp. 249–257, Dec. 2022, https://doi.org/10.15244/pjoes/153074.

[19] D. Yang, L. Yan, L. Yu, H. Yang, and P. Liao, "Abundance and characteristics of sediment-bound magnetic minerals and trace elements in karst ditch wetland: A case study from Guizhou Province, China," *Ecotoxicology and Environmental Safety*, vol. 243, Sept. 2022, Art. no. 113963, https://doi.org/10.1016/j.ecoenv.2022.113963.

[20] Q. Tao, Q. Zeng, M. Chen, H. He, and S. Komarneni, "Formation of saponite by hydrothermal alteration of metal oxides: Implication for the rarity of hydrotalcite," *American Mineralogist*, vol. 104, no. 8, pp. 1156–1164, Aug. 2019, https://doi.org/10.2138/am-2019-7043.

[21] M. Dumańska-Słowik, W. Heflik, A. Pieczka, M. Sikorska, and Ł. Dąbrowa, "The transformation of nepheline and albite into sodalite in pegmatitic mariupolite of the Oktiabrski Massif (SE Ukraine)," *Spectrochimica Acta Part A: Molecular and Biomolecular Spectroscopy*, vol. 150, pp. 837–845, Nov. 2015, https://doi.org/10.1016/j.saa.2015.06.039.

[22] S. Sudarningsih *et al.*, "Scanning Electron Microscopy and Magnetic Characterization of Iron Oxides in Suspended Sediments," *Indonesian Journal of Applied Physics (IJAP)*, vol. 14, no. 2, pp. 209–218, Nov. 2024, https://doi.org/10.13057/ijap.v14i2.76582.

[23] O. Rasulov, M. Schwarz, A. Horváth, F. Zoirov, and N. Fayz, "Analysis of soil contamination with heavy metals in (the three) highly contaminated industrial zones," *SN Applied Sciences*, vol. 2, no. 12, Nov. 2020, Art. no. 2013, https://doi.org/10.1007/s42452-020-03813-9.

[24] C. Su *et al.*, "Heavy Metals in Soils From Intense Industrial Areas in South China: Spatial Distribution, Source Apportionment, and Risk Assessment," *Frontiers in Environmental Science*, vol. 10, Feb. 2022, https://doi.org/10.3389/fenvs.2022.820536.

[25] T. Shi *et al.*, "Status of cadmium accumulation in agricultural soils across China (1975–2016): From temporal and spatial variations to risk assessment," *Chemosphere*, vol. 230, pp. 136–143, Sept. 2019, https://doi.org/10.1016/j.chemosphere.2019.04.208.

[26] M. Radziemska and J. Fronczyk, "Level and Contamination Assessment of Soil along an Expressway in an Ecologically Valuable Area in Central Poland," *International Journal of Environmental Research and Public Health*, vol. 12, no. 10, pp. 13372–13387, Oct. 2015, https://doi.org/10.3390/ijerph121013372.

[27] C. Matara, S. Osano, A. O. Yusuf, and E. O. Aketch, "Prediction of Vehicle-induced Air Pollution based on Advanced Machine Learning Models," *Engineering, Technology & Applied Science Research*, vol. 14, no. 1, pp. 12837–12843, Feb. 2024, https://doi.org/10.48084/etasr.6678.

[28] V. B. Kadam, A. V. Tejankar, and S. K. Sirsat, "The Study of Heavy Metal Contamination in Industrial Soils of Aurangabad Using GIS Techniques," *Journal of Geomatics*, vol. 17, no. 1, pp. 53–61, Apr. 2023, https://doi.org/10.58825/jog.2023.17.1.73.

[29] P. S. Harikumar, U. P. Nasir, and M. P. M. Rahman, "Distribution of heavy metals in the core sediments of a tropical wetland system," *International Journal of Environmental Science & Technology*, vol. 6, no. 2, pp. 225–232, Mar. 2009, https://doi.org/10.1007/BF03327626.

[30] S. Salim, R. S. Mohammed, and I. M. Kareem, "Assessment of Heavy Metal Contamination of Groundwater in Rural Areas of Duhok City, Iraq," *Engineering, Technology & Applied Science Research*, vol. 14, no. 4, pp. 15149–15153, Aug. 2024, https://doi.org/10.48084/etasr.7501.

[31] B. A. Maher, "Magnetic properties of some synthetic sub-micron magnetites," *Geophysical Journal International*, vol. 94, no. 1, pp. 83–96, July 1988, https://doi.org/10.1111/j.1365-246X.1988.tb03429.x.